HyperWatch: A Stratospheric Infrared Search-and-Track Layer for Hypersonic Missile Defense

Technical White Paper

Brian Check

July 2025

Contents

1 Problem & Operational Need

China's hypersonic glide vehicles such as the DF-ZF, flying above Mach 5 at low altitudes with unpredictable maneuvers, can evade traditional radar and satellite sensors. Without persistent, fire-control-quality tracking over regions like Guam and the Taiwan Strait, U.S. forces face strategic surprise.

Ground-based radars are limited by Earth's curvature and terrain, requiring expensive, geographically constrained deployments that only marginally extend horizon reach. Space-based IR sensors view targets through a warm atmospheric column and incur high background flux, short integration times, and orbit-driven custody gaps - making the delivery of fire-control-quality tracking data for interceptor guidance extremely challenging and unreliable.

The urgent need is for a persistent, wide-area thermal surveillance layer that overcomes these geometry-driven limitations at affordable cost and with rapid surge capability in strategic theaters.

2 HyperWatch Concept Overview

HyperWatch fills this gap with a network of 20 km-altitude balloons carrying stabilized IRST payloads. This network:

- **Extends reach**: 20 km elevation nearly doubles detection horizon without terrain constraints, further amplified to 4× when station-keeping offshore (Sec. 3).
- **Boosts sensitivity**: Up-look through cold stratospheric sky yields hundreds of times higher per-frame SNR than LEO down-look (Sec. 4). This margin enables precise centroiding, low false-alarm rates, and continuous high-confidence tracks—meeting the accuracy demands of fire-control-quality tracking.
- **Ensures regional persistence**: Superpressure balloons station-keep for 100+ days using differential wind layers. Unlike satellites locked to orbital paths, they can loiter over fixed areas of interest—such as Guam—for the full duration of a conflict. Existing HGVs are built for regional, theater-range attacks. Wars are fought in regions; coverage must be too.
- **Cost effective**: Delivers coverage at a fraction of the cost of expensive GEO or LEO constellations.
- **Rapidly deployable**: Launches in under 1 hour from truck or ship; scalable coverage can be surged to new regions without the lead times or orbital constraints of space assets.
- **Adds a resilient layer**: Distributed and attritable, HyperWatch can rapidly restore coverage if primary sensors are jammed, degraded, or destroyed, ensuring continuity in contested environments.

By combining stratospheric geometry with IRST physics and networked processing, HyperWatch provides the missing surveillance layer for hypersonic defense.

3 Coverage & Reaction Time Gains vs. Ground Radar

Raising the sensor even tens of kilometers above the surface fundamentally changes how early an incoming threat can be detected. The benefit comes from simple Earth curvature: line–of–sight

distance to a target at altitude grows with the *square root* of sensor height. A modest vertical lift therefore produces a disproportionately large horizontal reach, which translates directly into added decision and intercept time.

3.1 Geometry Fundamentals

For a spherical Earth of radius R_E and two points at altitudes h_1 (sensor) and h_2 (target), neglecting refraction, the maximum mutual line–of–sight range is

$$R_{12} = \sqrt{(R_E + h_1)^2 - R_E^2} \; + \; \sqrt{(R_E + h_2)^2 - R_E^2} = \sqrt{2R_E h_1 + h_1^2} + \sqrt{2R_E h_2 + h_2^2}. \tag{1}$$

For $h \ll R_E$ (true for stratosphere and HGV altitudes),

$$R_{12} \approx \sqrt{2R_E h_1} + \sqrt{2R_E h_2}. \tag{2}$$

Thus each additional meter of sensor altitude returns diminishing but still valuable horizontal reach: $dR/dh \propto 1/\sqrt{h}$.

3.2 Single Balloon vs. Sea-Level Radar (Illustrative Case)

Parameters:

$$R_E = 6371 \text{ km}, \quad h_2 = 30 \text{ km (HGV)}, \quad h_1^{\text{radar}} = 0 \text{ km}, \quad h_1^{\text{balloon}} = 20 \text{ km}.$$

Sea-level radar horizon to 30 km target:

$$R_{0,30} \approx \sqrt{2R_E h_2} = \sqrt{2 \times 6371 \times 30} \approx 617 \text{ km}.$$

20 km balloon to same target:

$$R_{20,30} \approx \sqrt{2R_E \cdot 20} + \sqrt{2R_E \cdot 30} \approx 510 + 617 = 1127 \text{ km}.$$

Coverage extension factor: $1127/617 \approx 1.83\times$ (an 83% increase in early detection radius with only a 20 km vertical lift).

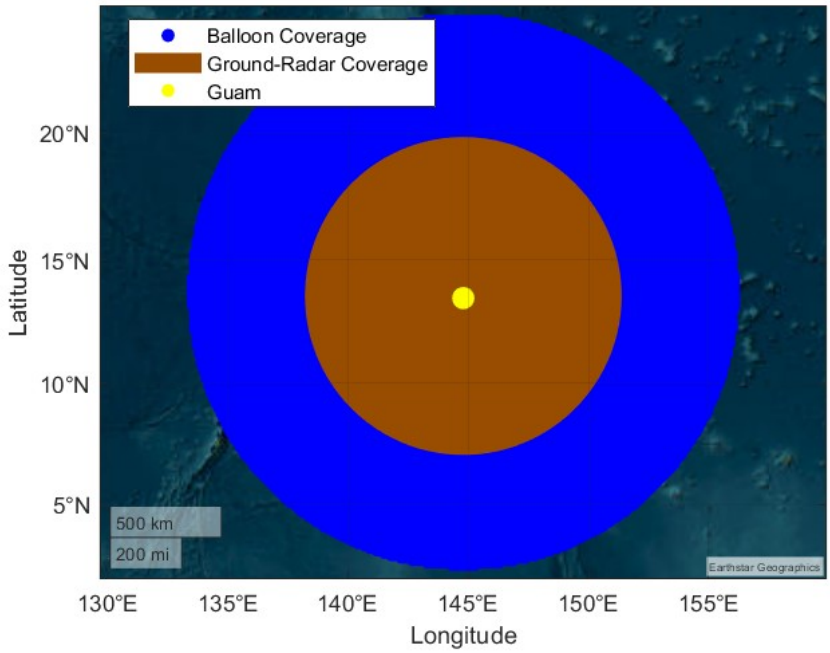

Figure 1: Single balloon line-of-sight coverage compared to ground radar (terrain effects not shown).

This geometric advantage becomes even more pronounced when terrain is considered, as mountains, coastlines, and urban clutter severely constrain ground radar visibility, especially against low-flying threats. For now, we assume a smooth Earth to isolate the pure geometric gain and highlight the fundamental advantage of the elevated sensor.

3.3 Networked Ring (Guam Example)

A single platform extends reach; a *ring* multiplies it. Consider 12 balloons roughly evenly spaced on a circle of radius $R_{\text{ring}} = 1000$ km, station-keeping offshore. Each balloon has an outward line-of-sight reach to the target altitude band (HGV at 30 km) of

$$R_{\text{balloon}\to\text{tgt}} \approx 1127 \text{ km}$$

The effective outer early-warning radius from the defended center is then

$$R_{\text{outer}} \approx R_{\text{ring}} + R_{\text{balloon}\to\text{tgt}} \approx 1000 \text{ km} + 1127 \text{ km} = 2127 \text{ km}.$$

Relative to the sea-level radar horizon to a 30 km target (617 km), this is a radial engagement distance increase of 3.45×.

Thus, the composite early-warning "fence" more than triples the defended radius and pushes initial detection well beyond 2000 km. Overlapping balloon footprints form a contiguous shell and allow for rapid dual-site angle–angle triangulation (cross-bearing "fixes") that fuse simultaneous bearings into an accurate 3-D passive track.

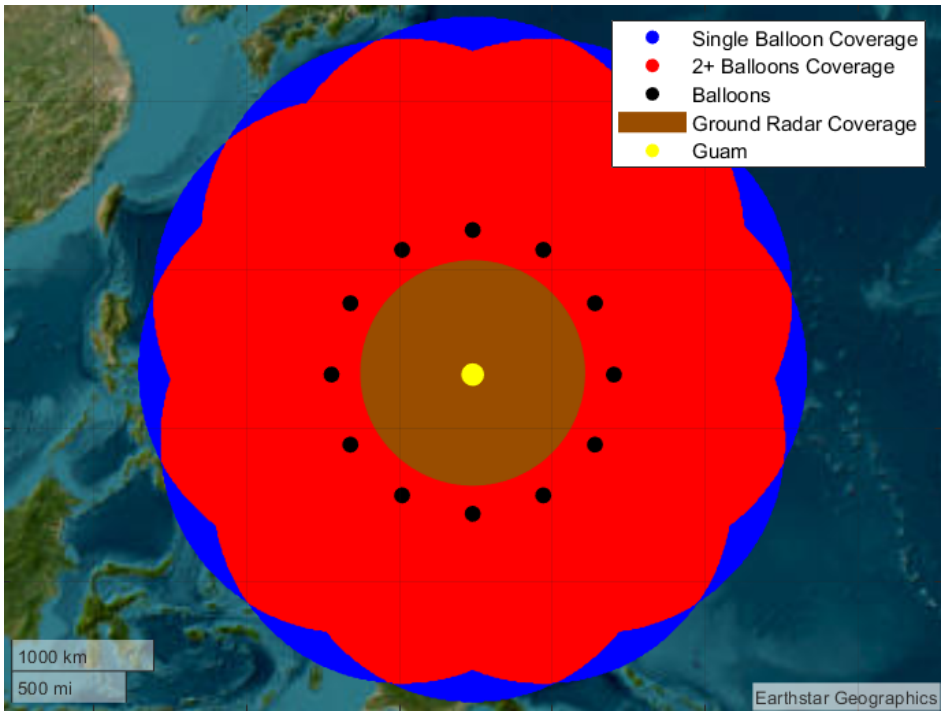

Figure 2: Twelve-balloon coverage ring (Guam concept).

3.4 Reaction Time Gain

Extended detection range is only part of the advantage. What matters operationally is the time it buys, extra seconds or minutes to track, decide, and engage. We now quantify how this geometric gain translates into actionable reaction time.

For a first estimate, assuming constant speed, if the threat cruises at $v = \text{Mach } 7 \approx 2.36\ \text{km/s}$, then the time from detection to impact is:

$$t_{\text{radar}} = \frac{617\ \text{km}}{2.36\ \text{km/s}} \approx 261\ \text{s}\ (4.4\ \text{min}),$$

$$t_{\text{balloon,single}} = \frac{1127\ \text{km}}{2.36\ \text{km/s}} \approx 477\ \text{s}\ (8.0\ \text{min}), \quad t_{\text{balloon,network}} = \frac{2127\ \text{km}}{2.36\ \text{km/s}} \approx 901\ \text{s}\ (15.0\ \text{min}).$$

This 15-minute "outer-fence" detection corresponds to a detection radius that is 3.45× greater than that of sea-level radar and nearly double that of a single balloon. The added

$$\Delta t_{\text{network}} = t_{\text{balloon,network}} - t_{\text{radar}} \approx 640\ \text{s}\ (10.7\ \text{min})$$

of warning time enables earlier classification, decision-making, and layered interceptor cueing.

Beyond the Constant-Speed Approximation. Real hypersonic glide trajectories decelerate due to drag; speed may fall from Mach 8 toward Mach 5–6 across midcourse, which *lengthens* actual reaction time compared to the constant-speed estimate. Our internal trajectory model (see Appendix A) integrates drag and adaptive glide shaping; Figure 3 shows reaction time contours vs. the missile's initial speed and cruise altitude, highlighting that the balloon network sustains roughly **triple the reaction time** over all plausible profiles.

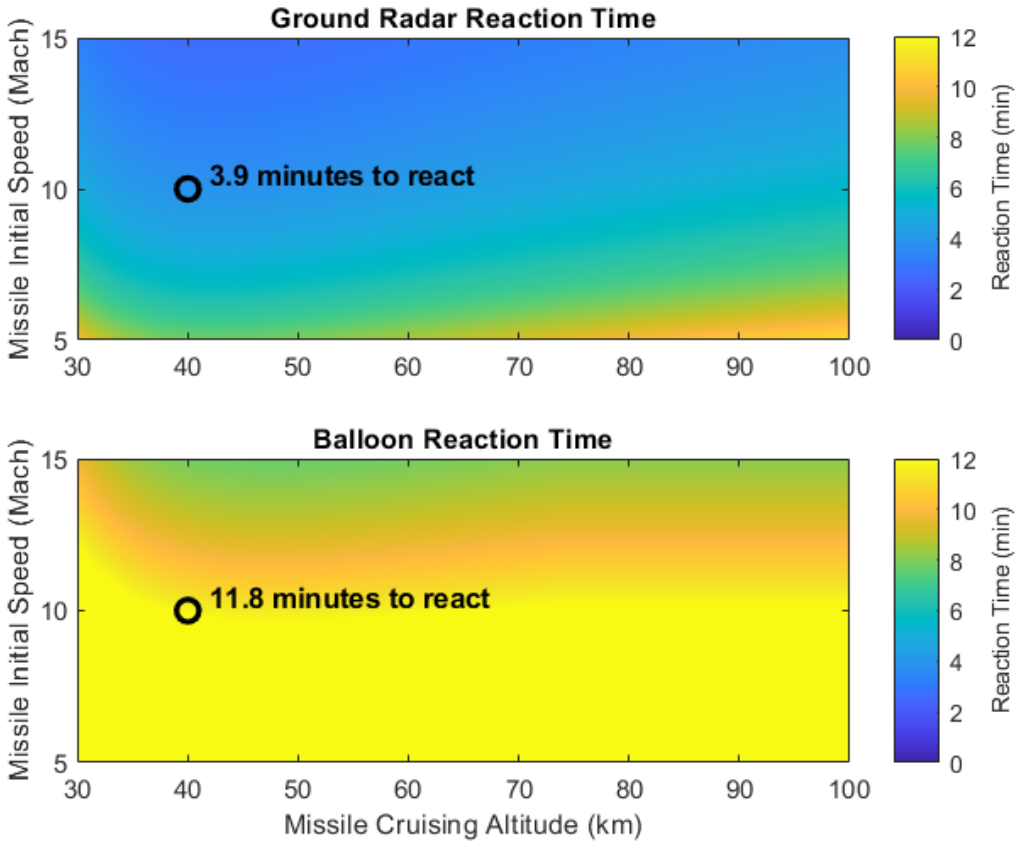

Figure 3: Reaction (tracking) time comparison across glide vehicle initial speeds and cruise altitudes.

3.5 Why the Added Minutes Matter

Additional minutes are not cosmetic; they reshape the engagement geometry:

- **Target characterization**: With extra lead time, IR sensors can capture several high-SNR frames before the missile maneuvers, enabling precise estimation of its trajectory curvature, thermal signature, and crucially, identification of the missile type for tailored countermeasures.
- **Interceptor tailoring**: Having detailed data on the inbound missile's speed and signature allows selection of the correct interceptor, flight profiles, and seeker modes optimized for that specific threat.
- **Fire–assess–fire**: Spacing intercept attempts by a few minutes lets operators evaluate each shot's outcome, adjust firing solutions on the fly, and thus raise overall kill probability while conserving interceptor inventory.
- **Cueing refinement**: Early, reliable IR tracks dramatically narrow down the search volume for follow-on radar or satellite systems, speeding up subsequent lock-on and reducing overall sensor handover delay.

Elevating a passive IR sensor into the stratosphere forms a concrete operational leverage: nearly doubling single-node reach and multiplying warning time; scaling a dozen nodes into a regional

early-warning shell; and delivering high-SNR tracks early enough to enable layered, adaptive defense. This is the geometric and temporal backbone the Golden Dome requires.

4 Radiometric and SNR Advantage of Stratospheric IRST

4.1 Introduction and Motivation

The hardest part of hypersonic defense is maintaining a high-confidence track while a boost-glide vehicle cruises at 40 km, well before terrestrial radar achieves line-of-sight. A stratospheric balloon infrared search and track (IRST) at 20 km "looks up" into cold, thin air; a LEO satellite (750 km) must "look down" through the whole atmospheric column onto a bright 300 K Earth background. That contrast / path geometry difference directly drives signal, background, permissible integration time, and thus signal-to-noise ratio (SNR). HyperWatch exploits (a) dramatically shorter range, (b) higher atmospheric transmission over a short slant path, and (c) a colder, lower radiance background enabling longer integrations to charge-well limits.

4.2 Step-by-Step Radiometric & SNR Algorithm

In this section we quantify the improvement in SNR obtained by placing an IRST sensor in the stratosphere instead of in orbit. We use a broadband LWIR band (8.0–10.1 µm) radiometric model following Driggers [1].

All calculations are available in our public MATLAB scripts `irst_calc_point.m` (single case) and `irst_snr_range_dual.m` (range sweep) [2].

For both cases (space and stratospheric sensor positioning), the following computations were performed to calculate their SNR.

1. **Slant-range** R between the object and the sensor

$$R = \sqrt{(R_e + z_s)^2 + (R_e + z_t)^2 - 2\,(R_e + z_s)(R_e + z_t)\cos\Big(\frac{\Delta_{\text{arc}}}{R_e}\Big)}.$$

2. **Atmospheric transmission** τ_{atm} Interpolate the band-averaged LWIR transmission along that path:

   - Up-look (20–40 km): $\tau_{\text{atm}} \approx 0.976$
   - Down-look (surface→750 km): $\tau_{\text{atm}} \approx 0.800$

3. **Target stagnation temperature** T_{tgt}

$$T_{\text{tgt}} = T_\infty \left[1 + r\,\frac{\gamma - 1}{2}\,M^2\right],$$

   where $r \approx 1.0$, $\gamma = 1.4$, $M = 8$, and T_∞ is ambient static temperature obtained from an atmospheric model.

4. **Band-integrated radiances**

$$B(\lambda, T) = \frac{2hc^2}{\lambda^5}\,\frac{1}{\exp\!\big(\frac{hc}{\lambda k T}\big) - 1}, \quad L(T) = \int_{\lambda_{\min}}^{\lambda_{\max}} B(\lambda, T)\,d\lambda,$$

   then compute $L_{\text{tgt}} = L(T_{\text{tgt}})$, $L_{\text{bg}} = L(T_{\text{bg}})$ for $T_{\text{bg}} = 220$ K (sky) or 290 K (Earth).

5. **Differential irradiance**
$$E_{\text{diff}} = \frac{A_{\text{tgt}}}{R^2}\,\tau_{\text{atm}}\,(L_{\text{tgt}} - L_{\text{bg}}).$$

6. **Pulse Visibility Factor (PVF)** A system-level coefficient accounting for optics blur and fill factor. Inputs are f-number (F), average wavelength λ
$$\text{PVF} = 0.0335\,e^{-0.887\,F\lambda/d_{\text{cc}}} + 0.9665.$$

7. **Signal electrons**
$$n_{\text{sig}} = \frac{\pi D^2}{4}\,E_{\text{diff}}\,\tau_{\text{opt}}\,\text{PVF}\,\frac{\lambda_{\text{ave}}}{hc}\,\text{QE}\,t_{\text{int}}.$$

8. **Background electron rate** With $E_{\text{bg}} = \frac{A_{\text{pix}}}{R^2}\,\tau_{\text{atm}}\,L_{\text{bg}}$:
$$\dot{n}_{\text{bg}} = \frac{\pi D^2}{4}\,E_{\text{bg}}\,\tau_{\text{opt}}\,\text{PVF}\,\frac{\lambda_{\text{ave}}}{hc}\,\text{QE}.$$

9. **Integration time** (well-fill control)
$$t_{\text{int}} = \min\Big(t_{\text{cap}},\,\frac{f_{\text{fill}}\,W}{\dot{n}_{\text{bg}}}\Big).$$

10. **Total background electrons**
$$n_{\text{bg}} = \dot{n}_{\text{bg}}\,t_{\text{int}}.$$

11. **RMS noise**
$$N_{\text{rms}} = \sqrt{n_{\text{bg}} + n_{\text{lens}} + n_{\text{dk}} + n_{\text{read}}^2}\,.$$

12. **Per-frame SNR**
$$\text{SNR} = \frac{n_{\text{sig}}}{N_{\text{rms}}}.$$

Table 1. Sensor Specifications

Parameter	Symbol	Value	Units
Aperture diameter	D	28.3	mm
f-number	$F/\#$	1.5	—
Pixel pitch	d_{cc}	15	µm
Quantum efficiency	QE	0.75	—
Optical transmission	τ_{opt}	0.70	—
Well capacity	W	1.2×10^7	e-
Design fill fraction	f_{fill}	0.65	—
Integration cap	t_{cap}	1.7×10^{-3}	s
Band limits	—	8.0–10.1	µm
Average wavelength	λ_{ave}	9.05	µm

Table 2. Computed Outputs

Quantity	Up-look (20 km)	Down-look (750 km)	Units
Slant range R	102	718	km
τ_{atm}	0.976	0.800	—
Target temp T_{tgt}	3465	3465	K
Background temp T_{bg}	220 K (sky)	290 K (Earth)	K
PVF	0.467	0.467	—
t_{int}	1.70×10^{-3}	2.71×10^{-4}	s
n_{sig}	8.17×10^{6}	2.17×10^{4}	e-
n_{bg}	9.48×10^{6}	7.80×10^{6}	e-
N_{rms}	3.24×10^{3}	2.96×10^{3}	e-
SNR	$\mathbf{2.52 \times 10^{3}}$	**7.32**	—

This representative scenario highlights the dramatic advantage of a stratospheric IRST for tracking a hypersonic glide vehicle. With otherwise identical sensors, HyperWatch (20 km up-look) achieves an SNR of 2,520, compared to 7.32 for the LEO down-look sensor - a factor of **344**× improvement in a single 1.7 ms integration.

4.3 SNR Across Operational Ranges

To demonstrate that this advantage holds across the full engagement envelope, we swept slant ranges from 10 km to 500 km. Figure 4 plots the per-frame SNR (log scale) for both HyperWatch and the LEO sensor:

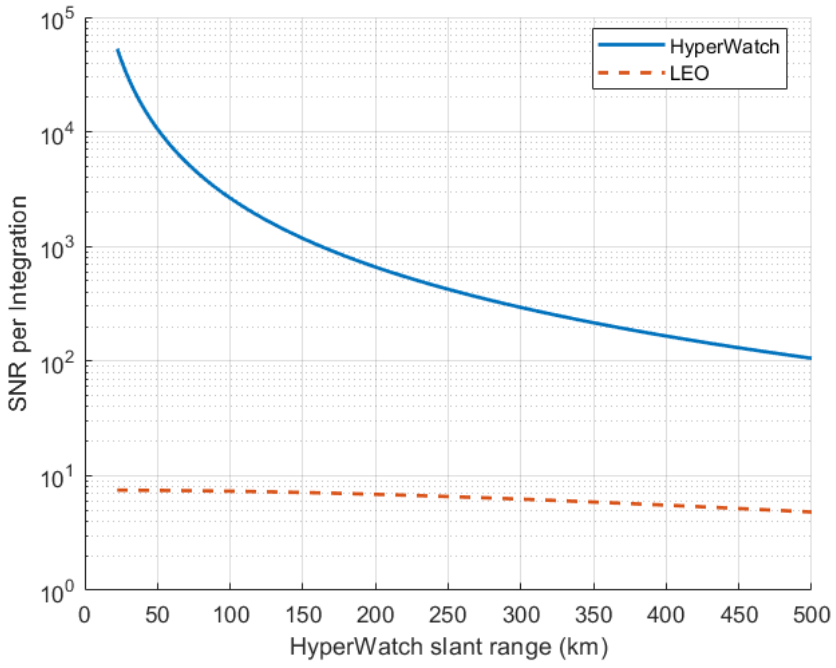

Figure 4: Per-frame SNR (log scale) vs. slant range: HyperWatch vs. LEO

Even in the most pessimistic case, when the balloon is 500 km away and the satellite is directly overhead, HyperWatch still maintains roughly a 15× SNR advantage over LEO. The down-looking LEO sensor never, at any range, exceeds an SNR of 10 (a common viability threshold for sub-pixel targets). At mission-critical ranges below 200 km, that advantage never drops below 100×, and at closer separations it soars into the thousands. Throughout the engagement envelope, the balloon platform consistently delivers long, cap-limited integrations with high SNR, whereas the spaceborne sensor's performance is sharply curtailed by background and range, making it unable to achieve even minimal detection thresholds at any point along the HGV's trajectory.

4.4 The Stratosphere is Better-Suited for HGV IRST than Space

This result is not "a modest improvement." It is a qualitative shift: we can now hold bright, high-confidence thermal track on a hypersonic glide vehicle *early and continuously*, well before ground radar clears the horizon, using a compact LWIR payload on a stratospheric platform. The physics are brutally simple: closer, cleaner, colder, and longer stare. Those four levers multiply; they are not incremental tweaks. Operationally, this means:

- **High track quality**: Massive per-frame SNR margin supports robust centroiding, discrimination, and low false-alarm thresholds.
- **Clean handoff**: Strong early tracks seed ground radar and space catalog correlation (the Golden Dome continuity we want), tightening the full kill chain.

A stratospheric up-look IRST layer turns a previously fragile early-track problem into a solvable, margin-rich sensing task and establishes the foundation of a fully operational hypersonic defense "dome."

Appendix

A Reaction-Time Plot Generation via HGV Simulation

To generate the reaction time contour plots, we simulate incoming hypersonic glide vehicle (HGV) trajectories across a range of initial speeds and cruising altitudes. For each speed–altitude pair, we calculate how much time a ground radar or a stratospheric balloon would have from first detection until missile impact.

The process involves two steps:

1. **Closed-Form Drag Calculation**
   For both the balloon and ground radar, we first calculate the line-of-sight detection range using Earth curvature geometry. Once detection range is known, we model the HGV's deceleration using an exponential drag formula based on altitude-dependent air density. Using this closed-form exponential drag model, we analytically solve for time-to-impact from detection point to ground. This produces approximate reaction times across the entire speed–altitude grid.

2. **Trajectory Integration Validation**
   To validate the closed-form results and capture realistic glide behavior, we also simulate full six-degree-of-freedom HGV trajectories using ordinary differential equation integration (ODE45 in MATLAB). This dynamic model includes position, velocity, altitude, heading, and flight path angle, with aerodynamic forces applied and a glide controller maintaining a target profile. The simulation terminates when the HGV reaches zero altitude. Reaction time is measured from detection range to this terminal event.

By comparing these two methods, we produce contour plots showing reaction time in minutes as a function of missile speed and altitude, separately for balloon-based and ground-based sensors. This directly quantifies how much extra warning time a stratospheric IRST would provide in different threat scenarios.

References

[1] R. G. Driggers, C. Lawrence, and E. J. Stevenson, *Introduction to Infrared and Electro-Optical Systems*, 3rd ed., Artech House, 2022. Chapter 17 discusses infrared search and track (IRST) systems.

[2] B. Check, "IRST," GitHub repository, 2025.
https://github.com/b9check/IRST